

## Article

# Seismic Behavior of Stone Pagoda Structure by Shaking Table Test

Ho-Soo Kim <sup>1</sup>, Dong-Kwan Kim <sup>1</sup>, Geon-Woo Jeon <sup>1,\*</sup>, Sang-Sun Jo <sup>2,\*</sup>, Se-Hyun Kim <sup>2</sup>

<sup>1</sup> Department of Architectural Engineering, Cheongju University, Cheongju, Republic of Korea

<sup>2</sup> National Research Institute of Cultural Heritage (NRICH), Daejeon, Republic of Korea

\* Correspondence: rjsdn1591@naver.com (G.-W.J.); ssjo@korea.kr (S.-S.J); Tel.: +82-43-229-8483 (G.-W.J); +82-42-860-9216 (S.-S.J)

**Abstract:** In general, the stone pagoda structures with discontinuous surfaces are vulnerable to lateral forces and are severely damaged by earthquakes. After the Gyeongju earthquake in 2016 and the Pohang earthquake in 2017, the earthquakes damaged numerous stone pagoda structures due to slippage, rotation and the separation of stacked stone. To evaluate seismic resistance of masonry stone pagoda structure, we analyzed the seismic behavior of stone pagoda structure using shaking table test. Shaking frequency, permanent displacement, maximum acceleration, rocking, and sliding were assessed. Responses to simulations of the Bingol, Gyeongju, and Pohang earthquakes based on Korean seismic design standard (KDS 41 17 00) were analyzed for return periods of 1,000 and 2,400 years. We found that the type of stylobate affected the seismic resistance of stone pagoda structure. When the stylobates were stiff, seismic energy was transferred from lower to upper regions of the stone pagoda, which mainly resulted in deformation of the upper region. When the stylobates were weak, earthquake energy was absorbed in the lower regions, which was associated with large stylobate deformations. The lower part of tower body was mainly affected by rocking, because the structural members were slender. The higher part of the stone pagoda was mainly affected by sliding, because the load and contact area decreased with height.

**Keywords:** Stone pagoda, Masonry structure, Shaking table test, Earthquake resistance, Seismic behavior

## 1. Introduction

The construction techniques used to create Korean stone pagodas, which are of great cultural importance, vary considerably. In general, stone pagodas with discontinuous surfaces are vulnerable to lateral forces and are severely damaged by earthquakes. After the Gyeongju Earthquake in 2016 ( $M_w=5.8$ ) and the Pohang Earthquake in 2017 ( $M_w=5.4$ ), conservation and management of Korean heritage became a major concern. The earthquakes damaged over 130 heritage structures due to slippage, rotation, and the separation of stacked stone. Some structural studies analyzing seismic behavior have suggested countermeasures, but dynamic tests that are applicable to various structural shapes are not available. Noh et al. (2002) [1] evaluated the earthquake responses of a half-scale, unreinforced masonry building via shaking table tests. Kim et al. (2011) [2] performed shaking table tests after reinforcing the inner and outer walls of structures, and suggested modifications that might improve seismic resistance. P. Gavrilovic et al. (1995, 2005) [3, 4] evaluated the seismic behavior of a 1/6-scale model of a Byzantine masonry church, and the effects of seismic reinforcement, using a shaking table. Fujita et al. (2006) [5] used shaking table tests to analyze the seismic behavior of a five-story wooden stupa. L. Kretevska et al. (2008) [6] evaluated the seismic resistance of mosques strengthened by fiber-reinforced plastic using a shaking table and finite element analysis. T. Hanazato et al. (2008) [7] analyzed the collapse of a masonry structure on a shaking table and performed discrete element analysis of a  $3 \times 3 \times 3$  m structure. Kim (2001) [8, 9] used a shaking table to evaluate the seismic behavior of the five-story Sang-Gye-Sa stone pagoda. Thus, most dynamic


experiments have explored masonry structures. However, stone pagodas increasingly being damaged by earthquakes, so more systematic analyses are required.

We used a shaking table to evaluate the seismic behavior of the three-story stone pagoda at Cheollyongsa temple site, which was damaged by the Gyeongju and Pohang earthquakes. Member composition type and the “Jeoksim” type were included among the experimental variables. The seismic wave was based on the Bingol earthquake, which is similar to the design response spectrum of the Korean building seismic design standard (KDS 41 17 00; 2019) [10], along with the Gyeongju and Pohang earthquakes. Deformation, the effects of seismic frequency, the maximum acceleration, permanent displacement, rocking, and sliding were analyzed.

2. The target structure

The three-story stone pagoda at Cheollyongsa temple site was severely damaged by the 2016 Gyeongju earthquake. The stone pagoda is 2.43 m wide and 7.24 m high (the decorative top starts at 4.8 m) and is a representative, single-stylobate stone pagoda of the late Unified Silla Dynasty. The stylobate is composed of 17 sheets, including the foundation stone, the main body comprising 6 sheets (1 for each story), and the upper part comprising 16 sheets (Table 1) [11].

Table 1. The three-story stone pagoda at Cheollyongsa temple site

Status	Classification		Member	Quantity (sheets)
	Upper part		Decorative top	16
	Body	3rd story	Roof stone	1
			Body stone	1
		2nd story	Roof stone	1
			Body stone	1
		1st story	Roof stone	1
			Body stone	1
		Foundation	Gapseok	4
			Myeonseok	8
	Foundation stone		5	
Total			39	

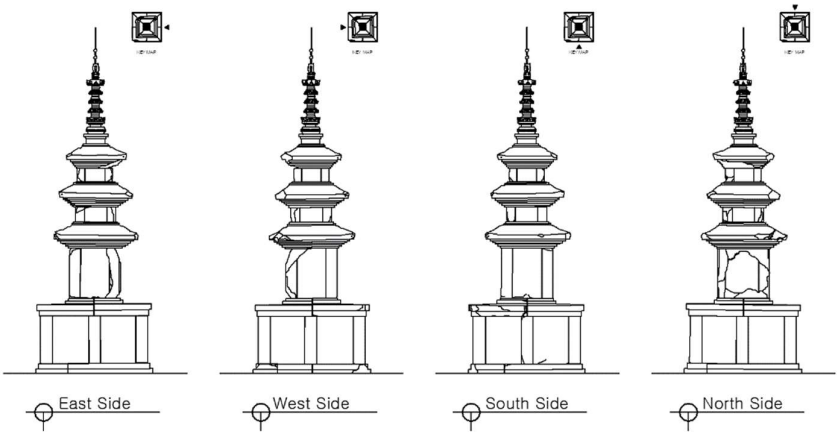


Figure 1. Views of the three-story stone pagoda at Cheollyongsa temple site

3. Experimental

3.1 Production of a scale model

We built a 1/3-scale model of the stone pagoda using high-quality rock with similar strength, absorption properties, surface roughness and member shape to the pagoda rock. The model dimensions are shown in Table 2 [12].

Table 2. Dimensions of the scale model of the stone pagoda based on the similarity law

Dimensions	Similarity law		Actual size	1/3-scale model
	Dimension	Exact scaling		
Width	L	$S_l$	2,430 mm	810 mm
Length	L	$S_l$	2,430 mm	810 mm
Height	L	$S_l$	4,750 mm	1,583 mm
Volume	V	$S_l^3$	12 m <sup>3</sup>	0.4 m <sup>3</sup>
Weight	W	$S_l^3$	274.4 kN	9.8 kN

To manufacture the experimental object, large rocks are cut to size and processed according to the shape and size of each member. The processed members are finished according to the roughness of the the three-story stone pagoda at Cheollyongsa temple site, and the size and condition are reviewed. Finally, the scale model is assembled.

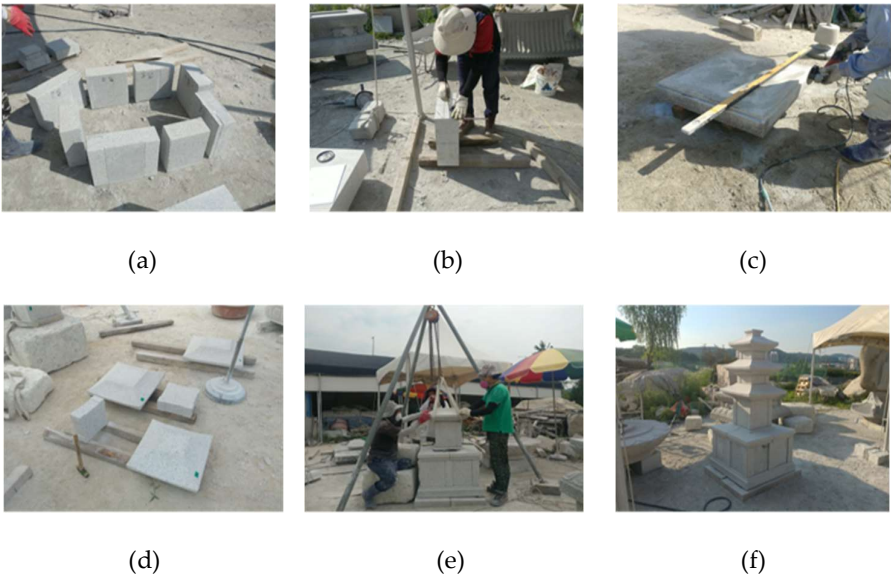


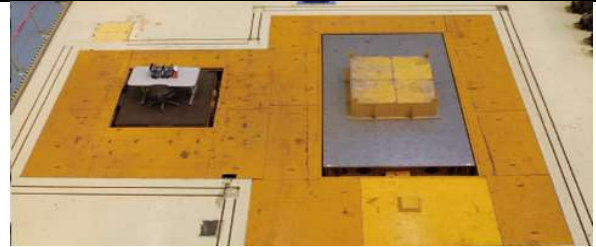
Figure 2. Photographs showing the model production process.: (a) Photograph of the members; (b) Cutting of the members; (c) Manufacturing process; (d) Review of the manufactured parts; (e) Provisional model assembly; and (f) The final model.

3.2 The shaking table

A two-axis shaking table was used (Hyundai Engineering & Construction Co., Ltd., Gyeonggi-do, Korea).; the maximum load was 50 kN, respectively, while the maximum vibration was 1 g and the maximum stroke was 75 mm, respectively [13].

**Table 3.** Shaking table specifications

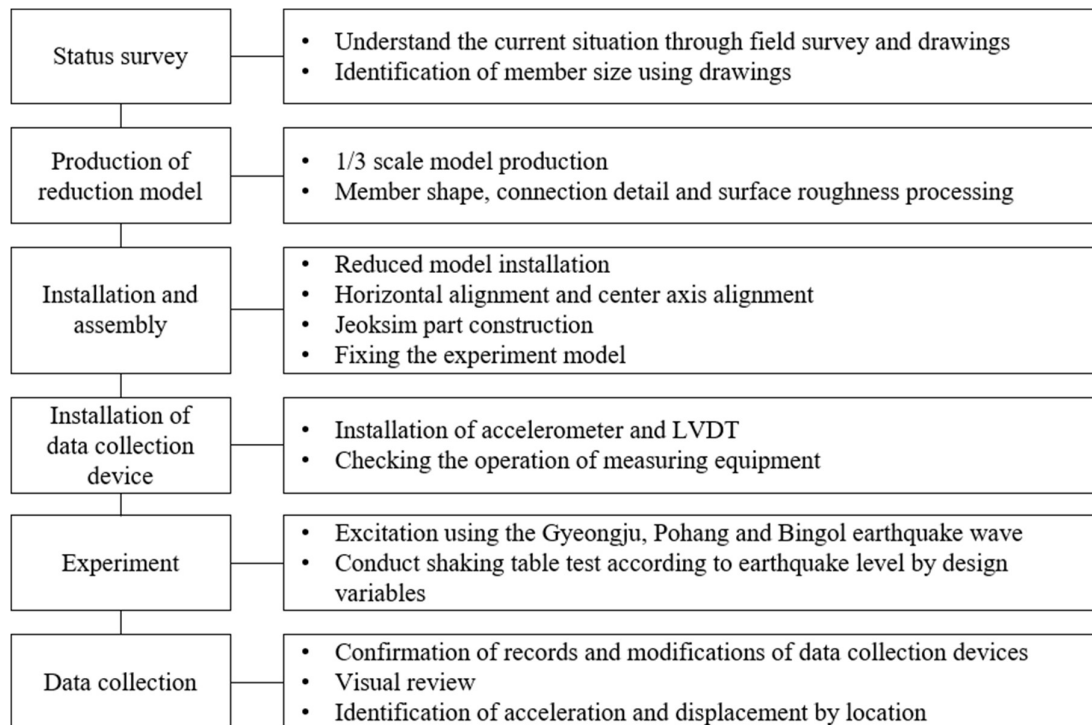
Parameter	One-axis	Two-axis
Size (m)	5 × 3	2 × 2
Load (kN)	300	50
Stroke (mm)	±100	±75
Speed (mm/s)	500	500
Maximum acceleration (g)	1.0	1.0



Shaking Tables (left: Two-axis, right: One-axis).

### 3.3 Method

The work plan is shown in Figure 3.

**Figure 3.** Details of the shaking table tests.

It was important not to damage the model during transport or assembly. When assembling the model, all contact surfaces were levelled to ensure a good fit. The shaking table and model were directly connected to prevent the model from slipping. The input acceleration, time, stress, and force data are shown in Table 4 [12].

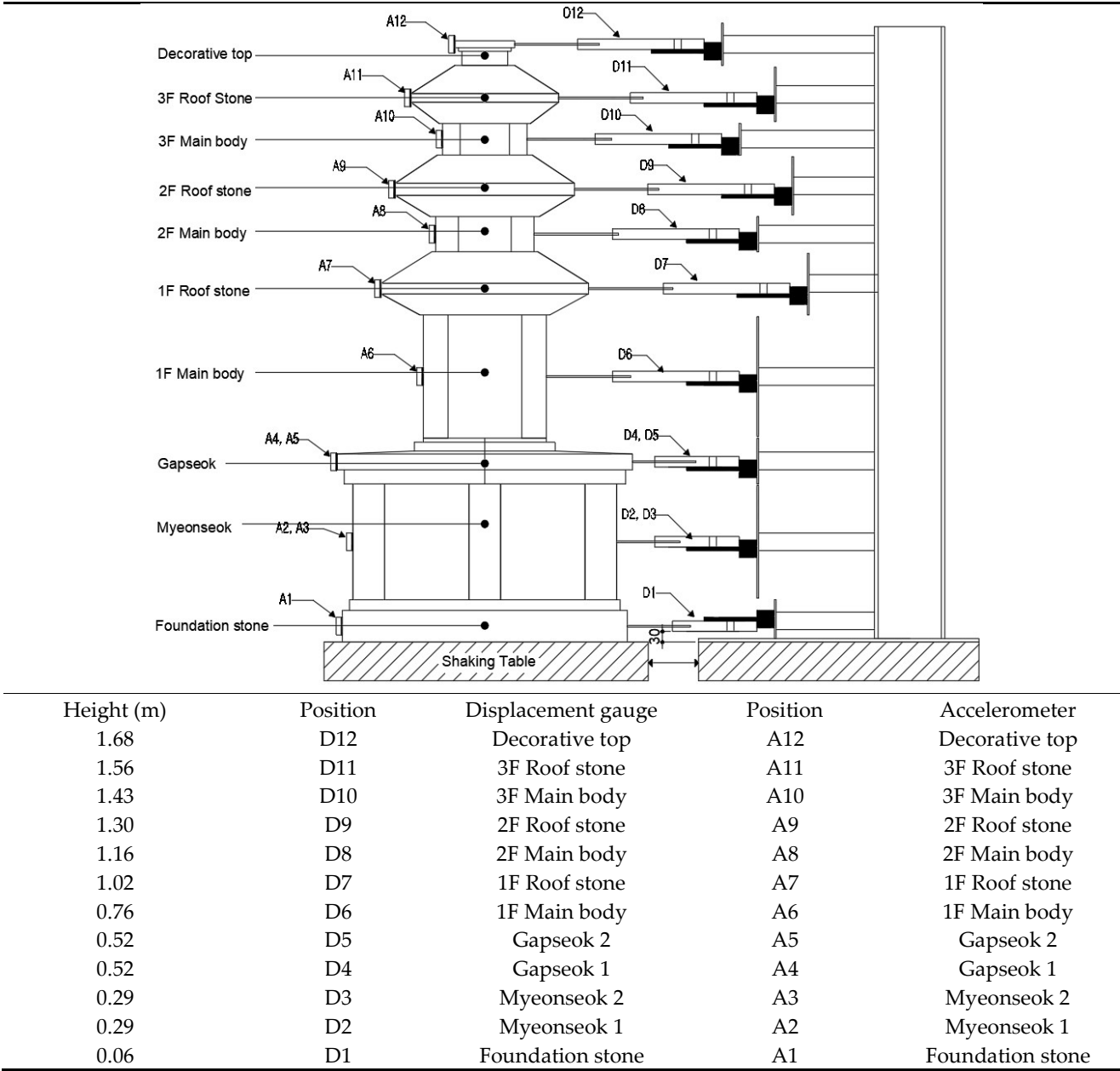
**Table 4.** The experimental conditions based on the similarity law

Variable	Length	Time	Acceleration	Stress	Force
Similarity	L	$\sqrt{T}$	1.0	$\sigma$	$F^3$
1/3-scale model	1/3	$1/\sqrt{3}$	1.0	1/3	1/27

### 3.4 Installation of measurement equipment

Displacement gauge/accelerometer units were installed on the foundation stone ( $n = 1$ ), Myeonseok ( $n = 2$ ), Gapseok ( $n = 2$ ), each main body stone and roof stone (all  $n = 1$ ), and the decorative top ( $n = 1$ ). All units were installed in the excitation direction, at the center of the member, and numbered.

Table 5. Measuring equipment installation locations



3.5 Experimental variables

The pagoda models were classified as Jeoksim<sup>1</sup> type A, Jeoksim type B, or loss of Jeoksim. Jeoksim A models were characterized by large, regularly stacked stones aligned along a central axis, and filled with soil and stone. The Jeoksim B model included irregularly stacked stones of various sizes compacted with soil. The loss of Jeoksim model was characterized by a partial loss of the stones in Jeoksim B type regions.

<sup>1</sup> Soil and gravel surrounded by stylobate stones.

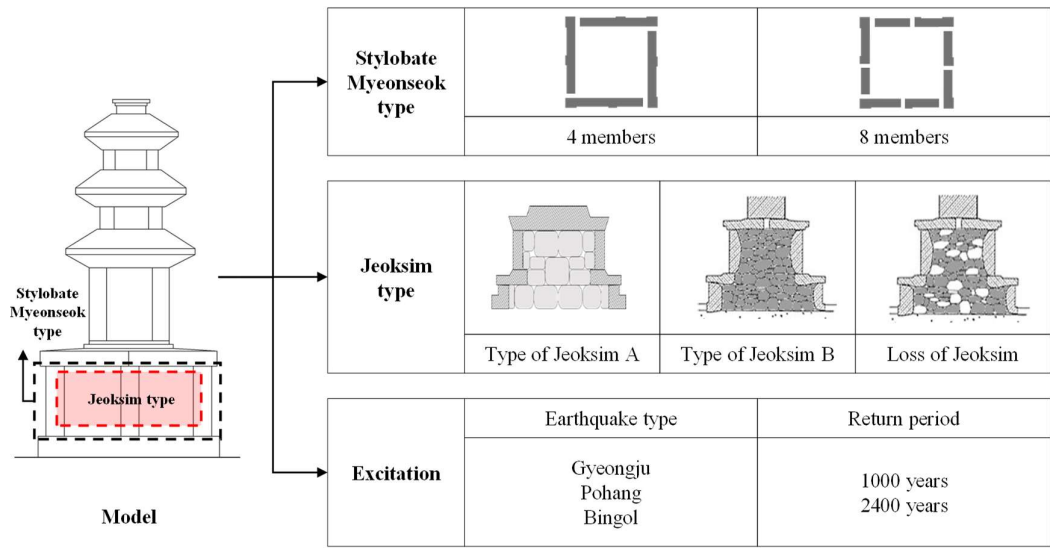


Figure 4. Schematic of a pagoda model and experimental variables.

The model types are detailed in Table 6. Figure 5 shows schematics of the Myeonseok and Gapseok.

Table 6. Experimental variables

Model type	Number of Myeonseok	Jeoksim type
Model 1 (basic model)	8	A
Model 2	4	A
Model 3	8	B
Model 4	8	Loss of Jeoksim

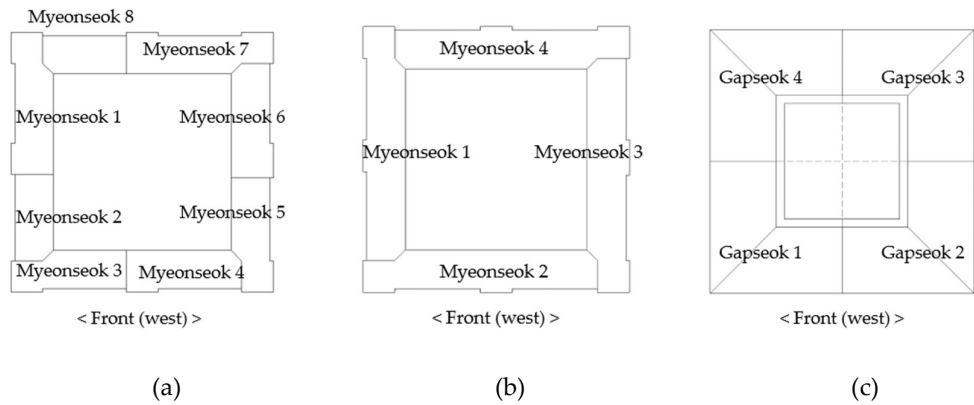


Figure 5. The Myeonseok and Gapseok: (a) Myeonseok included in models 1, 3, and 4; (b) Myeonseok included in model 2; and (c) Gapseok included in models 1-4.

3.6 Earthquake waves

We modeled the waves from the Gyeongju earthquake (2016), Pohang earthquake (2017), and Bingol earthquake (2003), based on the Korean seismic design standard (KDS 41 17 00; 2019). The return periods were 1,000 and 2,400 years.

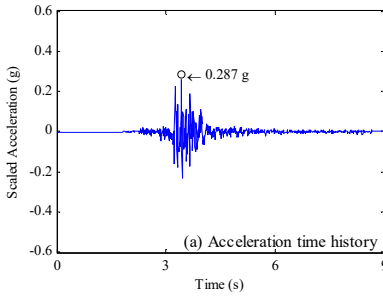
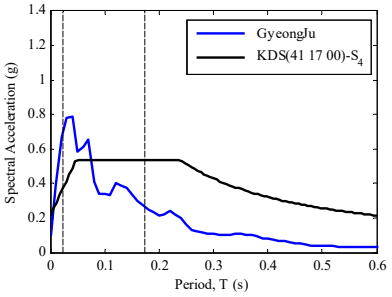
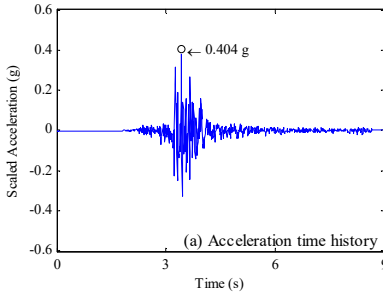
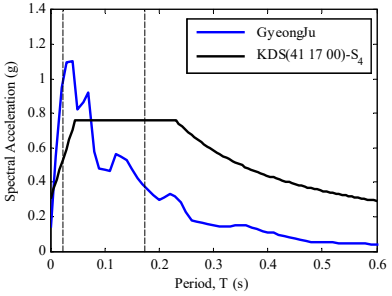
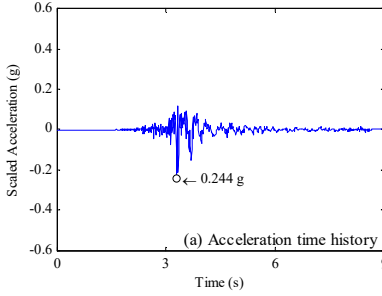
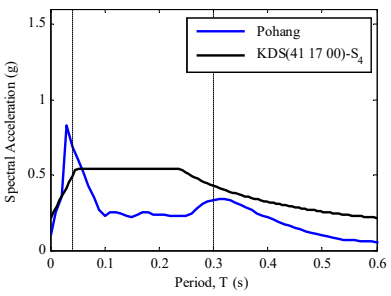
Table 7. Details of the simulated earthquakes

Earthquake	Year	Country	Station	Information		
				Magnitude	$R_{rup}^*$ (km)	Duration (s)
Gyeongju	2016	Korea	MKL	5.8	6	2.65
Pohang	2017	Korea	PHA2	5.4	9	2.8
Bingol	2003	Turkey	Bingol-Bayindirlik Murlugu	6.3	14	6.78

\*Distance between the epicenter and observation point.

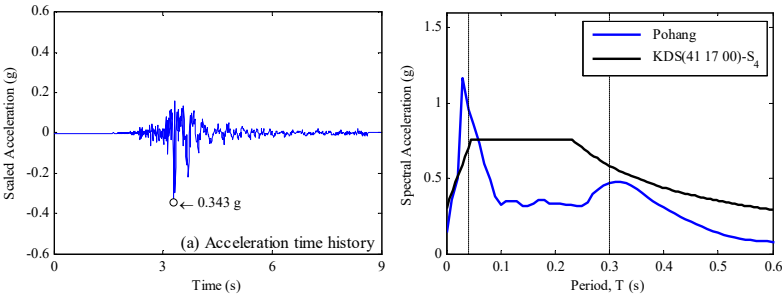
The effective ground acceleration and ground conditions were considered during wave modeling according to the KDS 41 17 00. As the structural period was reduced to  $1/\sqrt{T}$  by the similarity law, the period was reduced to  $1/\sqrt{3}$ . The details of the modeled seismic waves are provided in Table 8.

Table 8. Details of the earthquake waves

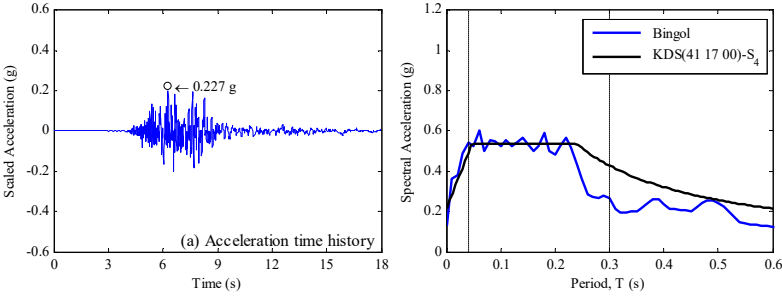
Earthquake	Return period	Earthquake wave	
Gyeongju	1,000 years (R1-G)		
	2,400 years (R2-G)		
Pohang	1,000 years (R1-P)		



2,400 years  
(R2-P)

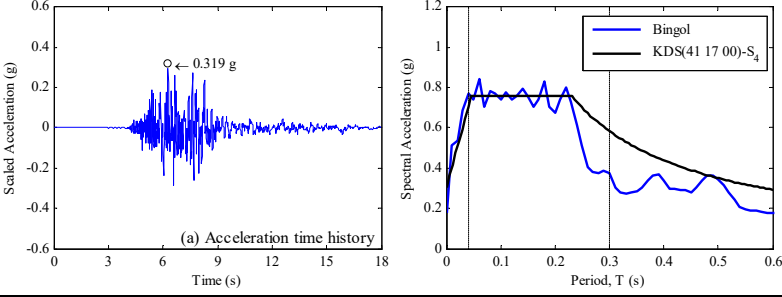


1,000 years  
(R1-B)



Bingol

2,400 years  
(R2-B)



4. Results

4.1 Deformation

The Myeonseok and Gapseok experienced the largest deformation; the main body of the stone pagoda was also rotated. Separation of the Myeonseok was minimal for models 1 and 2 [Jeoksim A). However, for models 3 [Jeoksim B; Figure 6(c)] and 4 [loss of Jeoksim; Figure 6(d)], separation of Myeonseok 6 and 7, on the righthand side, was the main type of deformation. Myeonseok 7 protruded to the rear (east). Seismic waves were delivered from the left (north) and right (south); the Myeonseok stones on the left and right were able to resist the forces due to the presence of the upper structure, and thus showed minimal deformation. However, the front and rear Myeonseok stones at right angles to the excitation direction were pushed out by the lateral pressure, indicating that the binding effect of the upper load was weak. Therefore, Myeonseok deformation was closely related to Jeoksim type; more regular and stable Jeoksim arrangements were associated with less stylobate deformation.



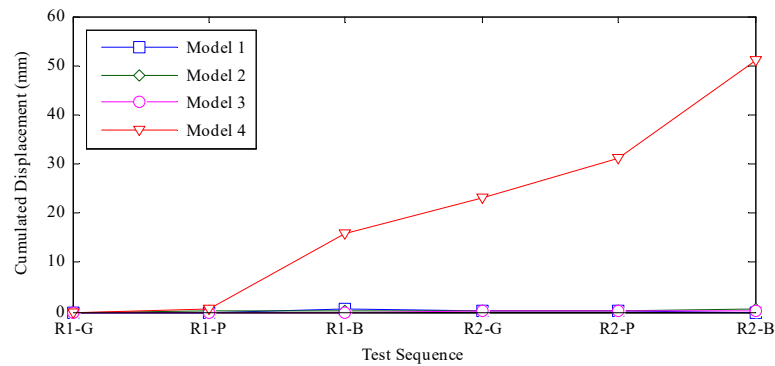
(a)

(b)

(c)

(d)





(e)

**Figure 6.** Images of Myeonseok deformation.:(a) Model 1; (b) Model 2; (c) Model 3; (d) Model 4; and (e) Cumulative displacement graph (for models 1, 3, 4, displacement occurred between Myeonseok 6 and 7; for model 2 displacement occurred between Myeonseok 3 and 4).

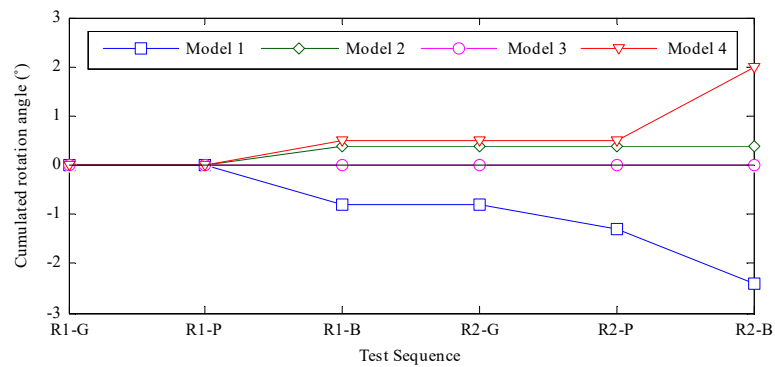
In addition, the first story of the main body of the tower was rotated counter-clockwise in models 1 and 3, while the second and third stories were rotated clockwise. All stories of the main body were rotated clockwise in model 2, and the first story of the main body in model 4. This result occurred because the loads acting on the tower differed by story. The roof stones tended to behave similarly to the main body stones.

The basic model 1 [Figure 7(a)] showed less deformation of the stylobate than models 3 and 4, but there was more rotational deformation of the tower body of model 1 than for the other models. For model 3 [Figure 7(c)], the Jeoksim type and stylobate deformation affected the deformation of the tower body. In model 2 [Figure 7(b)], in which four sheets of Myeonseok were affected, the generally stable stylobates reduced overall tower body deformation.

In summary, tower body deformation was affected by member configuration and Jeoksim type. The first-story main body stone is more slender than those of the second and third story, and therefore exhibited rotational deformation caused by rocking.



(a) (b) (c) (d)



(e)

**Figure 7.** Images showing the deformation of the main body stone in the various models.: (a) Model 1; (b) Model 2; (c) Model 3; (d) Model 4; and (e) Cumulative rotation angle of the first-story main body stone.

#### 4.2 Frequency analysis

Frequency can be analyzed based on the acceleration response spectra or by using the amplification function of the measured accelerations. However, for a stone pagoda, if frequencies are calculated only using the acceleration response spectra method, the values may be inflated, for example by rocking. Thus, we analyzed frequencies using both methods. Frequency is related to stylobate stiffness; reduced frequency means change or decrease in stiffness. The Bingol earthquake reduced stiffness more than the Gyeongju and Pohang earthquakes. For model 4, most seismic waves were very low frequency, because stylobate stiffness was reduced by the loss of Jeoksim. For model 3, the frequency with a return period of 1,000 years was lower than for the other models, while with a return period of 2,400 years, the frequency was similar to that of model 1. The frequency of the waves was higher for model 1 than models 3 and 4 over the short return period; for the longer period, the behavior was similar to that of model 3. As the return period increased, the frequency decreased sharply, attributable to rocking of the first story of the main body stone. Overall, model 2 was the least damaged.

**Table 9.** Frequency data for the four stone pagoda models

Return period	Earthquake	Model 1		Model 2		Model 3		Model 4	
		Period (s)	Frequency (Hz)	Period (s)	Frequency (Hz)	Period (s)	Frequency (Hz)	Period (s)	Frequency (Hz)
1,000 years	Gyeongju	0.111	9.00	0.109	9.13	0.109	9.13	0.108	9.27
	Pohang	0.093	10.80	0.105	9.53	0.118	8.47	0.100	10.00
	Bingol	0.123	8.10	0.101	9.90	0.169	5.90	0.171	5.85
2,400 years	Gyeongju	0.102	9.80	0.100	10.00	0.109	9.20	0.205	4.87
	Pohang	0.108	9.27	0.107	9.33	0.105	9.53	0.188	5.33
	Bingol	0.189	5.30	0.169	5.90	0.169	5.90	0.206	4.85

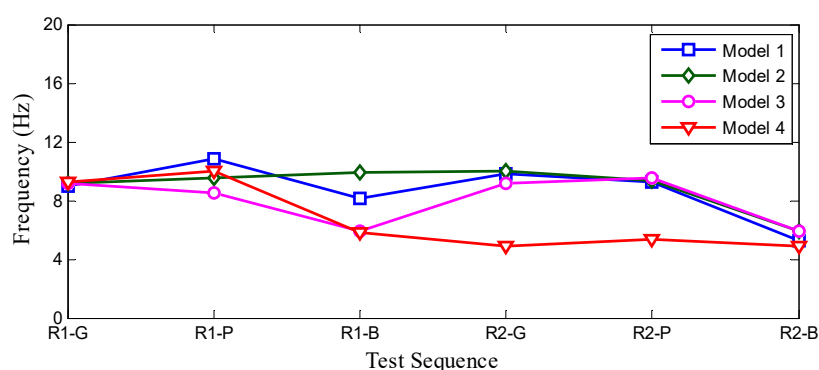


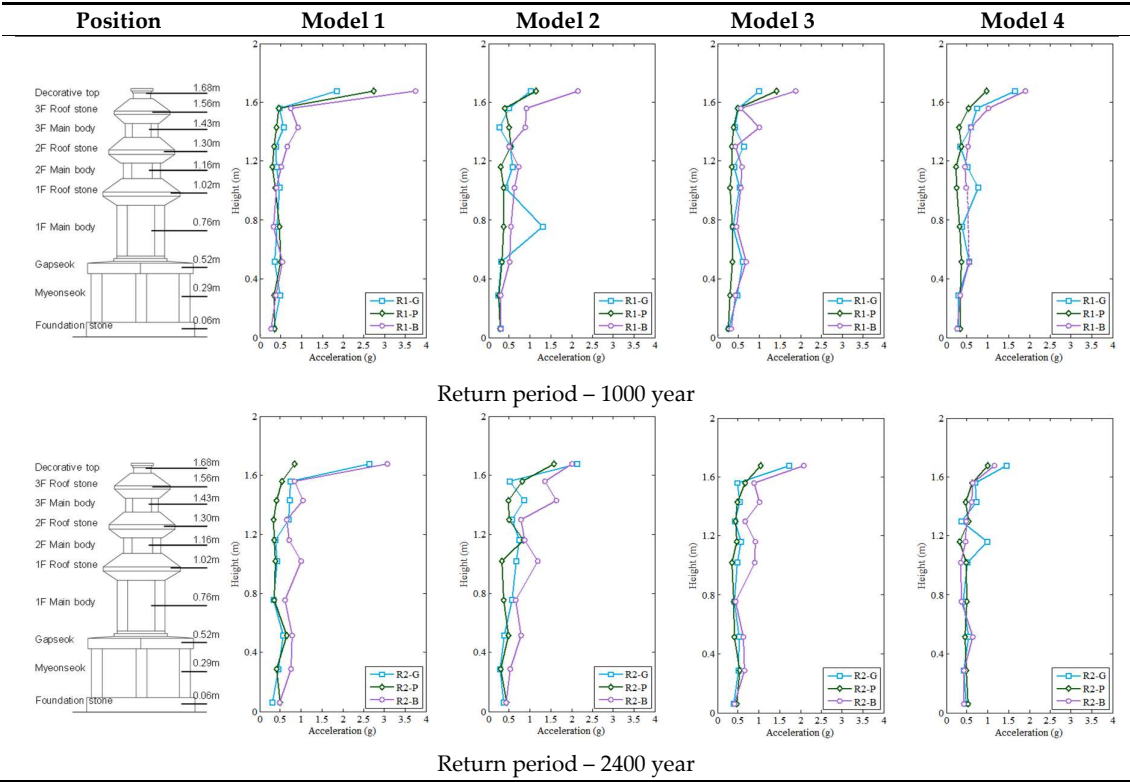
**Figure 8.** Frequency graphs for the four stone pagoda models.

#### 4.3 Maximum acceleration

Large changes in maximum acceleration were measured with a return period of 2,400 years rather than 1,000 years. For model 1, as the return period increased, the maximum acceleration also increased slightly, particularly for the decorative top and the Gapseok. Acceleration did not differ significantly among the other parts of the stone pagoda. The high acceleration at the decorative top was reflected in severe rocking, where the members are light in this part of the stone pagoda and the contact surface is unstable. Model 2 was similar to model 1, but the maximum acceleration was slightly lower. The discontinuous surface area of model 2 (four sheets of Myeonseok) was smaller than that of model 1 (eight

sheets), and the resistance to seismic load was accordingly higher. For model 3 (Jeoksim type B), the stylobate stiffness was relatively low compared to the Jeoksim type A models, but the maximum acceleration did not differ significantly. This is because the weight of the stone pagoda structure is mainly supported by the Jeoksim, so the seismic load is concentrated in the Jeoksim part. Maximum acceleration was not significantly measured in the Myeonseok or Gapseok. For model 4, the acceleration of both the Myeonseok and Gapseok was low due to their discontinuous surfaces, in turn caused by loss of Jeoksim. Also, the surface contact area of the Myeonseok and Jeoksim was smaller than in models 1 and 3. When comparing the behavior of the Myeonseok between models 4 (loss of Jeoksim) and 3 (Jeoksim type A), maximum acceleration was lower in model 4 because of the reduced lateral pressure exerted on the Myeonseok (in association with the lack of Jeoksim). Also, the maximum acceleration of the upper members (first and second story of the main body and roof stones, third story of the main body stone) was lower than that of the other models. This occurred because seismic energy was dissipated toward the top, and mainly deformed Myeonseok when stiffness was low because of the loss of Jeoksim.

Table 10. Acceleration data for all stone pagoda models

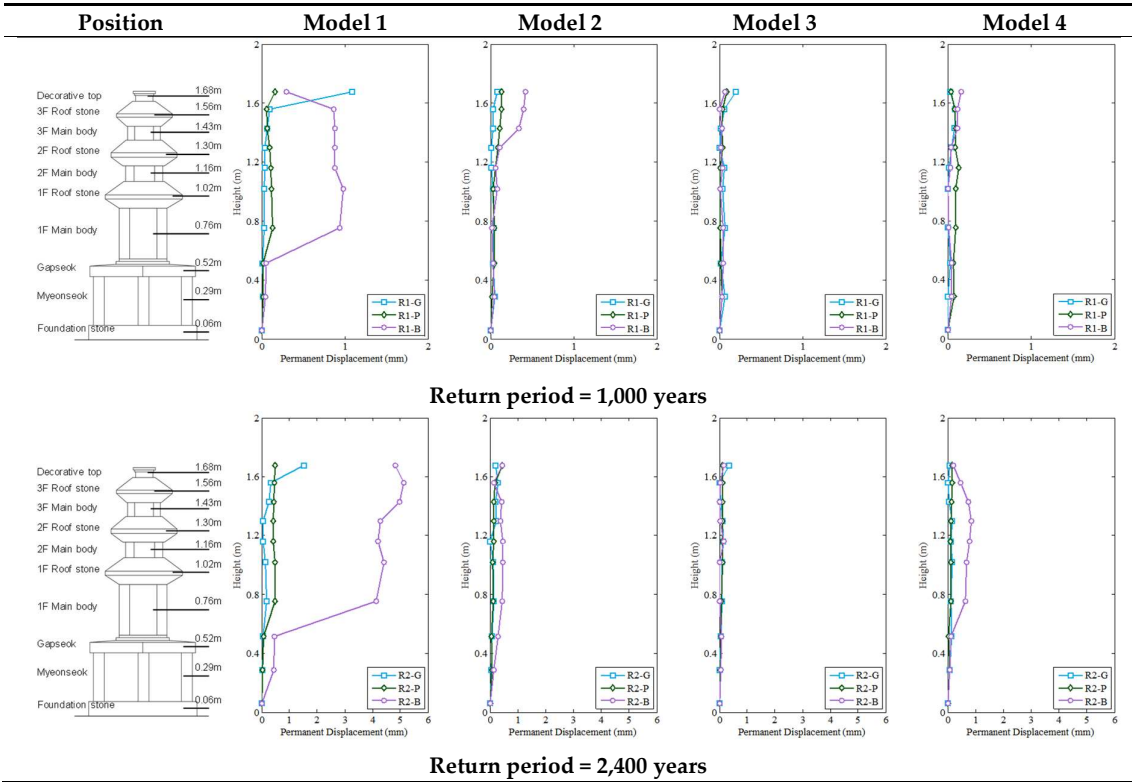


4.4 Permanent displacement

In model 1, permanent displacement of the first story of the main body stone was largest for the Bingol earthquake simulation; the stone was significantly rotated by rocking. For model 2, the overall displacement was not large. In most of the simulations, Myeonseok and Gapseok displacement did not occur. In model 2, the seismic load was relatively large due to the short vibration period. However, earthquake resistance was high due to the small discontinuous contact surface, so no permanent displacement occurred. For models 3 and 4, no obvious displacement of Myeonseok or Gapseok was evident; any displacement of Myeonseok stones was perpendicular to the direction of defor-

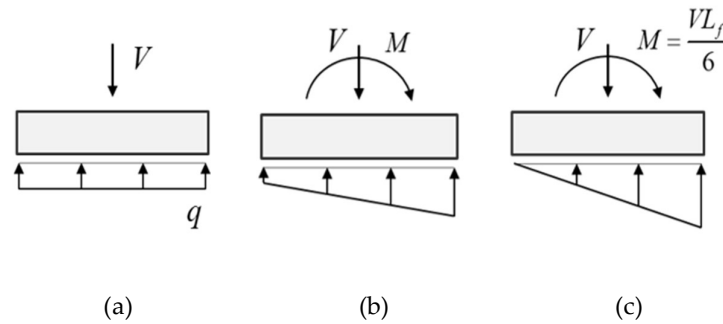
mation. Stylobate deformation was significant (2.5~20 mm) on the y-axis, due to the separation of Myeonseok, but not on the x-axis. Stylobate stiffness was lower when there was no Jeoksim, which greatly increased stylobate deformation.

Table 11. Permanent displacement data of the stone pagoda models



#### 4.5 Rocking

When only vertical loads were applied to unit member, the forces were compressive [Figure 9(a)] [14]. When the moments acted with the vertical loads, the load distributions were as shown in Figure 9(b). As the moments increased, the load distributions changed [Figure 9(c)]. When the compressive stress is zero on the left side and reaches its maximum value on the right side, a critical state without uplift develops. The moment in this state is the moment of the resistance force. In a triangular load distribution, the load is applied at  $1/3$  of the member width ( $L_f$ ); the distance from this point to the centroid is  $1/6$  of the member width. The moment resistance (overturning moment) of each member is given by equation (1).



**Figure 9.** Limitations on the uplift of members.: (a) Initial state; (b) Elastic state prior to uplift; and (c) Elastic state at uplift.

$$M_{uplift} = \frac{\sum_{n=1}^i W_n \times L_f}{6} \quad (1)$$

where  $W$  is the total weight between the upper and lower members, and  $L_f$  is the width of the contact surface of the bottom member.

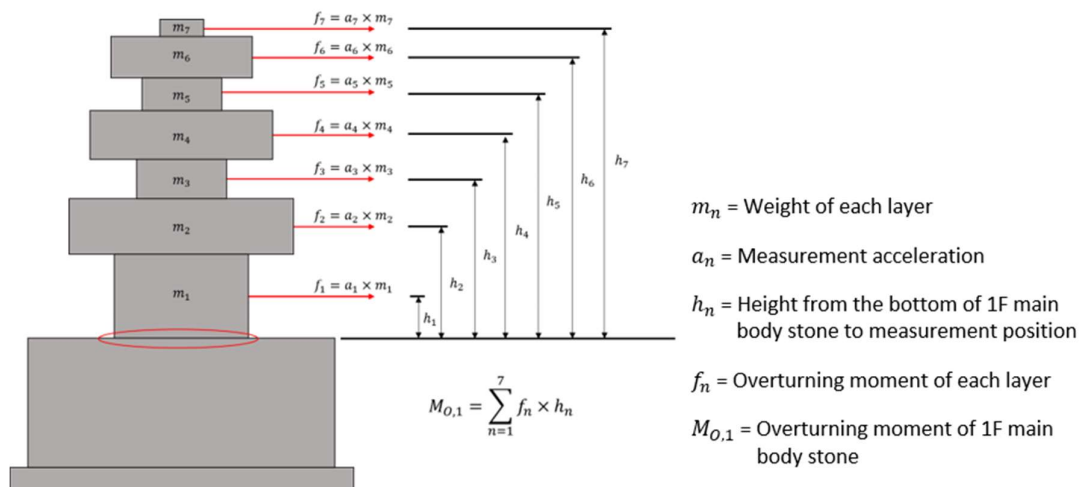
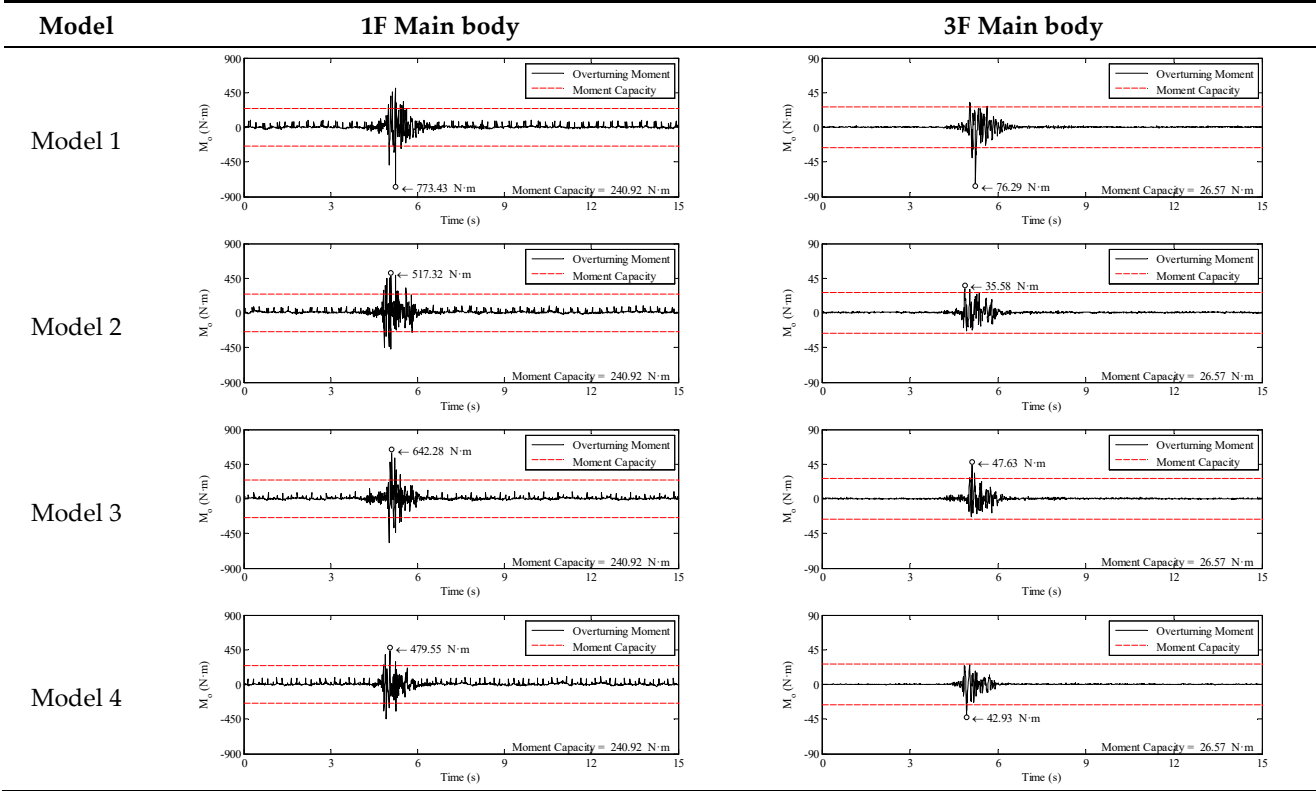


**Figure 10.** Calculation of the overturning moments.

The rocking analysis revealed that the moment resistance of the decorative top was very low, because the weight and area of the contact surface were very small compared to those of the other parts of the stone pagoda. However, for the slender first-story main body stone, the overturning moment greatly exceeded the moment resistance and rocking

occurred. We found no significant difference in the time of rocking occurrence between models 1 and 2. However, model 2 the maximum overturning moments of stories 1 and 3 were smaller. For the first-story main body stone, the probability of rocking was higher for model 1 than model 2. Therefore, resistance to overturning was lower when there were eight rather than four sheets of Myeonseok. For models 3 and 4, stylobate stiffness was lower than for model 1; upper-story shearing and the overturning moments decreased because vibration energy was dissipated by deformation of the stylobates.

Table 12. Rocking over time in the various stone pagoda models (return period 2,400 years; Gyeongju earthquake)



4.6 Sliding

The critical horizontal forces required for sliding are shown in Figure 10. Here, P is the vertical force acting on a block, H is the horizontal force, W is the weight, and  $\mu$  is the friction coefficient of the contact surface. The normal force (P) acting on a block is the sum of the weights of the members above the block. Here, the weight of the tower body is the same in all models. Sliding occurs when the story-shearing force exceeds a critical value. However, as  $\mu$  varies by the contact surface, it is difficult to estimate. We considered that sliding occurred when the maximum story-shearing force exceeded the horizontal force derived using a  $\mu$  value of 0.6.



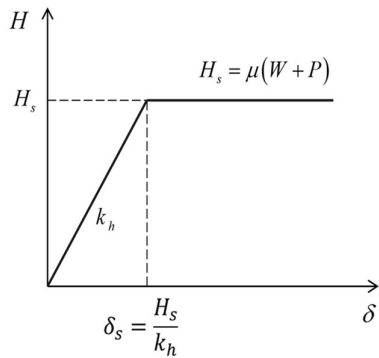


Figure 11. The critical horizontal force ( $H_s$ ).

The decorative top is very light and is not subjected to any loading force; thus, it slid during all earthquake simulations, for all return periods. Also, as the  $\mu$  value of 0.6 was exceeded by more members during the Bingol earthquake than the other earthquakes; it was associated with more sliding. For models 1, 2, and 3, sliding was mostly confined to the decorative top and third-story roof stone; for model 4, only the top slid for the return period of 2,400 years. In most models, sliding was reduced in lower regions because the self-weights and vertical loads increased sliding resistance.

Table 13. Sliding data for all stone pagoda models

Return period	Gyeongju	Pohang	Bingol
1,000 years			

5. Conclusions

We analyzed the seismic behavior of a 1/3 scale model of the three-story stone pagoda at Cheollyongsa temple site during earthquake simulation performed using shaking table

test. Deformation, maximum acceleration, permanent displacement, rocking, and sliding were evaluated.

With fewer Myeonseok stylobates, the discontinuous contact surface area was smaller and seismic performance was better. For the Jeoksim B and loss of Jeoksim models, the contact surface between Myeonseok and Gapseok decreased and stylobate stiffness also decreased, resulting in significant stylobate deformation. As most of the seismic energy transversely deformed the Myeonseok, damage was mainly seen in the lower region of the stone pagoda. In contrast, in the Jeoksim type A models, stylobate stiffness was relatively high, and rotational deformation (caused by rocking of the main body stones) was more significant than the deformation seen in the lower region. This mainly affected the first-story main body stone, leading to rotational deformation above that region.

The variation in maximum acceleration was greater for the longer return period, as was permanent displacement, rocking, and sliding. However, in terms of frequency, the seismic wave input was more important than the return period. Both the Gyeongju and Pohang earthquakes had short periods and relatively small deformation. The seismic duration was longest for the Bingol earthquake, and the response acceleration was therefore large. Therefore, the structure became more deformed, and the frequency decreased because of the reduced stylobate stiffness.

The Bingol earthquake caused the most sliding, mainly in the upper region. Both the self-weight and vertical loads reduced sliding in the lower region. Rocking of the decorative top was associated with a low overturning moment resistance; the top is very light and has minimal contact with other members. Also, the first-story main body tended to rock because of its slender members.

When stylobate stiffness is high, seismic energy received at the bottom of the pagoda is transferred upwards, which is associated with upper-region deformation. When stylobate stiffness is low, the Jeoksim absorbs most of the seismic energy, an effect associated with large stylobate deformation. In particular, the tower stone is strongly affected by rocking, because it becomes more slender toward the bottom. In contrast, sliding damage increases toward the top, because it is associated with a low applied load and minimal contact surface with lower members.

**Author Contributions:** Conceptualization, H.-S.K and S.-S.J; methodology, D.-K.K; software, G.-W.J and D.-K.K; validation, H.-S.K and S.-S.J; formal analysis, G.-W.J and D.-K.K; investigation, G.-W.J and S.-H.K; resources, S.-S.J and S.-H.K; data curation, G.-W.J and S.-H.K; writing—original draft preparation, G.-W.J and S.-S.J; writing—review and editing, G.-W.J and S.-S.J; visualization, G.-W.J and S.-H.K; supervision, H.-S.K; project administration, H.-S.K and S.-S.J; funding acquisition, H.-S.K

**Funding:** This research was carried out with the support of the Cultural Heritage Administration's National Research Institute of Cultural Heritage.

**Acknowledgments:** This research was carried out with the support of the Cultural Heritage Administration's National Research Institute of Cultural Heritage. The authors would like to express sincere gratitude for their support.

**Conflicts of Interest:** The authors declare no conflict of interest.

## References

1. Noh Hyun-Sup, Choi Sung-Mo, Kwon Ki-Hyuk, An Experiment Study on Dynamic Response of Two Story URM Buildings, *Journal of the Architectural Institute of Korea Structure & Construction*. 2002, 18, 59-66.
2. Kim Sang-Hyo, Choi Moon-Seock, Park Se-Jun, Ahn Jin-Hee, Seismic Performance Evaluation of Masonry Walls Retrofitted with Semi-buried Lattice Reinforcement *Journal of the Korea Institute for Structural Maintenance and Inspection*. 2011, 15, 88-98
3. P. Gavrilovic, V. Zelenkovska, W.S. Ginell, L. Sumanov, Development of a Methodology for seismic strengthening of Byzantine churches, *Transactions on the Built Environment*. 1995, 15, 37-44

4. P. Gavrilovic, V. Sendova, S.J. Kelley, Seismic isolation: a new approach to earthquake protection of historic monuments, Proc. of the IV International Seminar on Structural Analysis of Historical Constructions. 2005, 4, 1257–1264.
5. Kaori Fujita, Naohito Kawai, Chikahiro Minowa, Mikio Koshihara, Kazuki CHIBA, Shaking Table Test and Earthquake Response Monitoring of Traditional Japanese Timber Pagoda, Proceedings of the 9th World Conference on Timber Engineering, Portland. 2006, 207-214
6. L. Kretevska, L.J. Tashkov, K. Gramatikov, R. Landolfo, O. Mammana, F. Portioli, F.M. Mazzolani, Shaking Table Tests on the Large Scale Model of Mustafa Pasha Mosque without and with FRP, In Structural Analysis of historic construction. 2008, 383–391.
7. T. Hanazato, C. Minowa, T. Narafu, H. Imai, Qaisar Ali, K. Kobayashi, Y. Ishiyama, T. Nakagawa, Shaking Table Test of Model House of Brick Masonry for Seismic Construction, Proceedings of 14th World Conference of Earthquake Engineering (14WCEE). 2008,
8. Kim Jae-Kwan, Lee Won-Joo, Kim Young-Joong, Kim Byung-Hyun, Shaking Table Test of the Model of Five-story Stone Pagoda of Sang-Gye-Sa Mounted on Base Isolation Systems, Proceedings of Earthquake Engineering Society of Korea Conference. 2001, 1, 331-338
9. Kim Jae-Kwan, Ryu Hyeuk, Dynamic Test of a Full Scale Model of Five-Story Stone Pagoda of Sang-Gye-Sa, Journal of Earthquake Engineering Society of Korea. 2001, 5, 51-66
10. Ministry of Land, Infrastructure and Transport (MOLIT), Seismic Building Design Code (KDS 41 17 00: 2019), Sejong, Korea
11. National Research Institute of Cultural Heritage(NRICH), Stone pagoda of Gyeongsangbuk-do III; NRICH: Daejeon, Korea, 2009; p.149. (In Korean)
12. Hwang Jae-Seung, Hwang Jong-Kook, Dynamic Characteristics of Traditional Wooden Structure (Daeungjeon of Bongjeongsa) Excited by Historical Earthquake using Shaking Table, Journal of the Architectural Institute of Korea Structure & Construction. 2015, 31, 37-46
13. Lee Han-Seon, Jung Dong-Wook, Lee Kyung-Bo, Kim Hee-Cheul, Lee Young-Hak, Lee Ki-Hak, Survey of Experimental Research Performed using Shaking Table Tests for Buildings in Korea, Proceedings of Korea Concrete Institute Conference. 2008, 1-4
14. Dong-Kwan Kim, Hong-gun Park, Dong-Soo Kim, Hyerin Lee, Nonlinear system identification on shallow foundation using Extended Kalman Filter, Soil Dynamics and Earthquake Engineering. 2020, 128, 1-12